Electronic Supplementary Material (ESI) for Journal of Materials Chemistry C.

Supporting Information

A PA66 lamellae crystal film with excellent triboelectric performance in vertical contact separation mode

Jincheng Liu[1,2], Po Ji[1,2], Zixun Wang[3], Xianglan Liu[2], Yongxing Lin[2,] Xiangyang Li[2], Lin Chen[2], Xingyou Tian[2], Sihai Luo[4,*]*

[1] Institutes of Physical Science and Information Technology, Anhui University, Hefei, Anhui, 230601, People's Republic of China.

[2] Key Laboratory of Photovoltaic and Energy Conservation Materials, Institute of Solid State Physics, Hefei Institutes of Physical Science, Chinese Academy of Sciences, Hefei, Anhui, 230031, People's Republic of China.

[3] School of Materials Science and Engineering, Energy Materials and Devices Key Lab of Anhui Province for Photoelectric Conversion, Anhui University, Hefei, Anhui, 230601, People's Republic of China.

[4] Department of Chemistry, Norwegian University of Science and Technology (NTNU), 7491, Trondheim, Norway

*Corresponding Authors: yxlin@issp.ac.cn, sihai.luo@ntnu.no.

Fig. S1 Jincheng Liu et al.

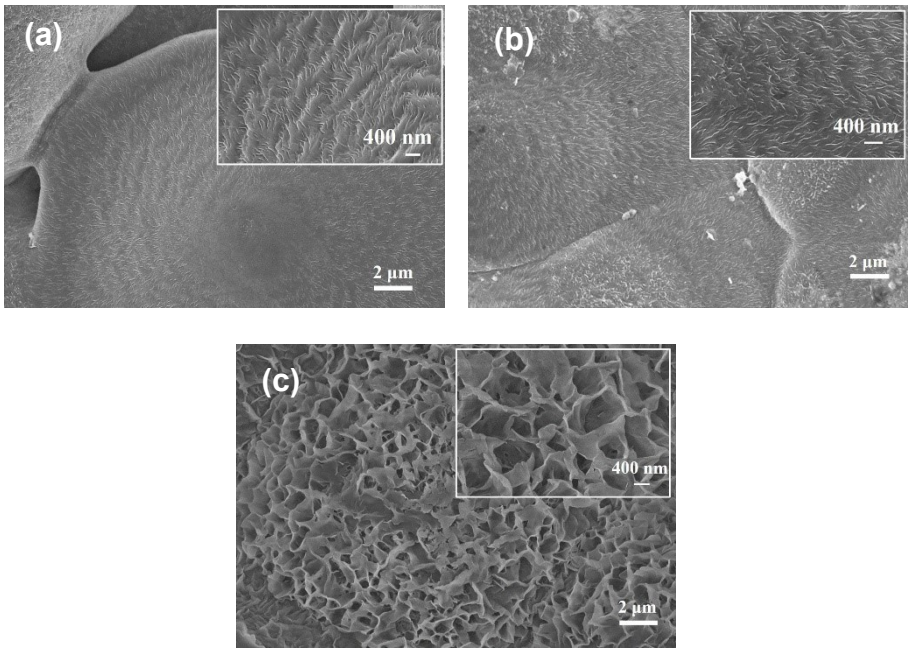

Fig. S1 SEM images of the surface morphology of the PA66 films at different temperatures in 0.2 wt% PA66 incubation solution: (a) 120 °C, (b) 130 °C, and (c) 150 °C. Insets are local images with high magnification.

Fig. S2 Jincheng Liu et al.

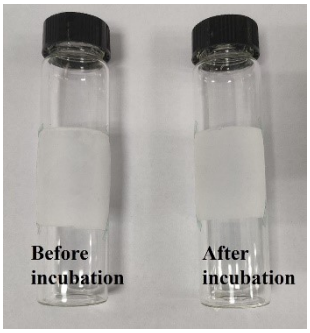

Fig. S2 Photograph of PA66 spin-coated film before and after incubation.

Fig. S3 Jincheng Liu et al.

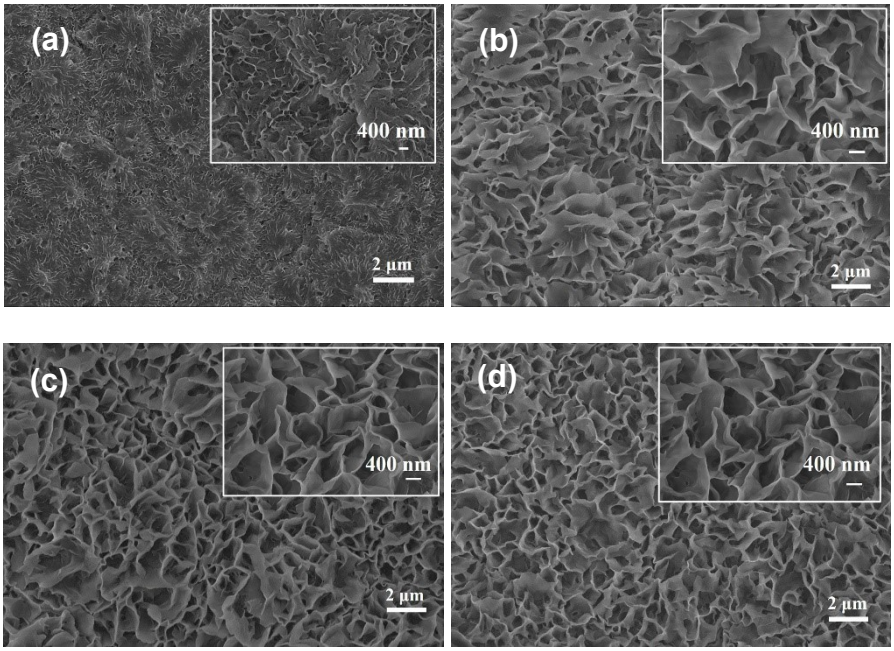

Fig. S3 SEM images of the surface morphology of the PA66 films for different incubation times in 0.2 wt% PA66 incubation solution: (a) 10 min, (b) 1 h, (c) 1.5 h, and (d) 2 h. Insets are local images with high magnification.

Fig. S4 Jincheng Liu et al.

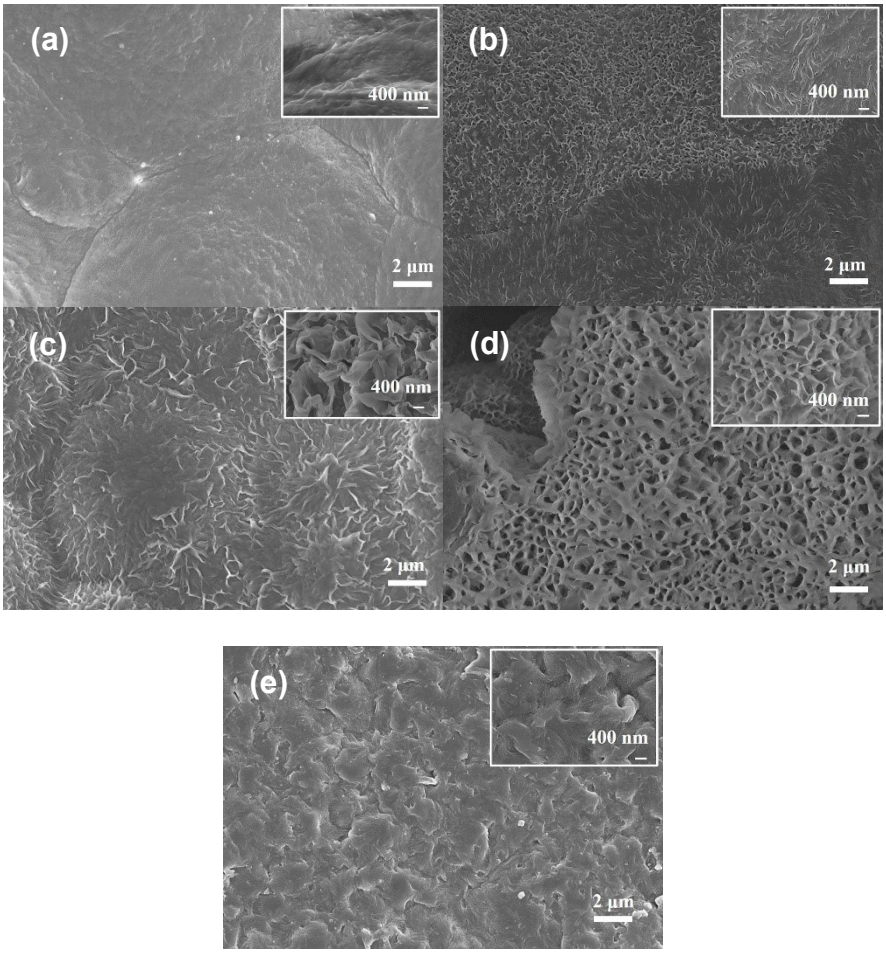

Fig. S4 Surface SEM images of the PA66 films in different PA66 incubation solutions (140 °C，30 min): (a) 0 wt%, (b) 0.01 wt%, (c) 0.05 wt%, (d) 0.1 wt%, and (e) 0.3 wt%. Insets are local images with high magnification.

Table S1 Jincheng Liu et al.

Table S1 Crystallinity index data for the initial PA66 spin-coated film and structural PA66 film incubated at various concentrations.

Samples	Crystallinity/%
Initial PA66	21.43
0.01 wt%	23.31
0.05 wt%	24.72
0.1 wt%	26.59
0.2 wt%	35.67
0.3 wt%	22.64

Fig. S5 Jincheng Liu et al.

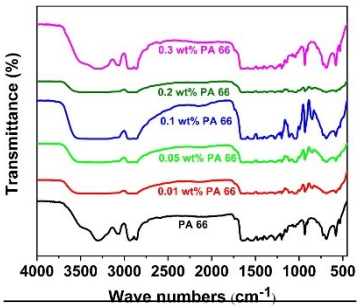

Fig. S5 FTIR spectra of pure PA66 spin-coated film and PA66 lamellae-crystal films at various incubation concentrations.

Fig. S6 Jincheng Liu et al.

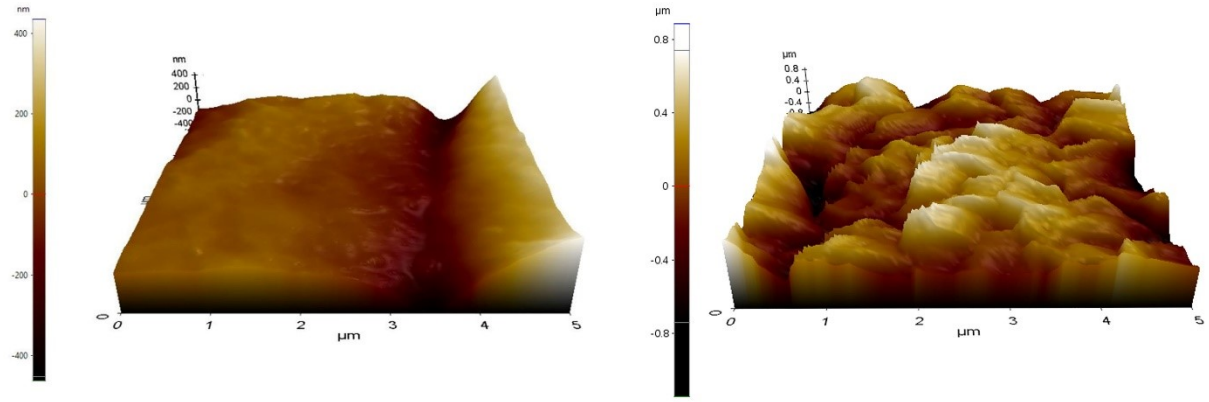

Fig. S6 AFM images of (a) pure PA66 spin-coated film and (b) PA66 lamellae-crystal film.

Fig. S7 Jincheng Liu et al.

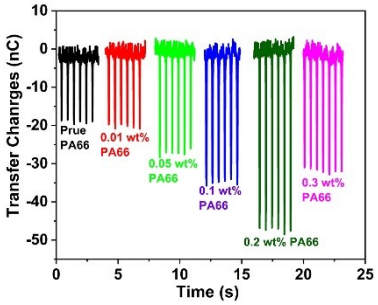

Fig. S7 Transfer charge quantities of TENGs based on pure PA66 spin-coated film and PA66 lamellae-crystal structure films incubated in several incubation solution concentrations.

Fig. S8 Jincheng Liu et al.

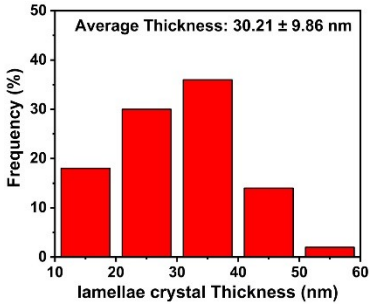

Fig. S8 Histogram of the thickness distribution of the lamellae crystal.

Fig. S9 Jincheng Liu et al.

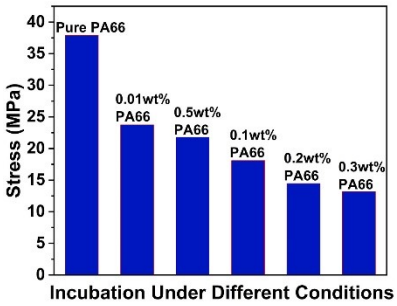

Fig. S9 Stress of the initial PA66 spin-coated film and PA66 lamellae crystal films as a function of incubation concentrations.

Fig. S10 Jincheng Liu et al.

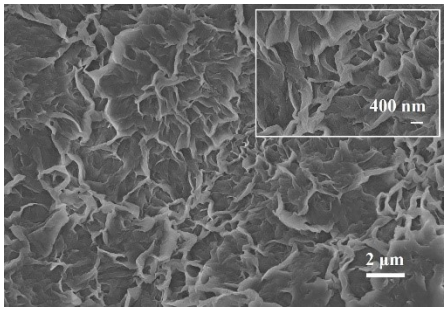

Fig. S10 The surface morphology of PA66 lamellae crystal film after 10,000 seconds of impact at 2 Hz.

Table S2 Jincheng Liu et al.

Table S2 LC-TENG performance compared to previously reported triboelectric nanogenerators.

Reference	Materials (Friction Layers)	Output Voltage (V)	Output Current (μA)	Power Density (W/m^2)	Tapping force (N)	Sensitivity (V/F)	Operation frequency (Hz)
(1)	electrospun nylon 66-Silk & /PVDF-PET	101	9.34	0.28	8	121.625	8
(2)	electrospun PA66 nanofiber & electrospun P(VDF-TrFE) nanofiber	166	8.5	0.093	200	0.83	5
(3)	PA66-Ag yarn & PTFE-Ag yarn	32	1.9	0.0075	-	-	3
(4)	patterned PVDF membranes and patterned nylon membranes	~120	~6.0	0.23	~78.4	~1.5306	2.85
(5)	PA66/MWCNTs nanofibers film & electrospun PVDF nanofibers film	142	15.5	1.5	15	9.4667	5
(6)	nylon & Silicone Rubber	1170	138	11.2	100	11.7	3
(7)	electrospun PA66 nanofiber & Ni-	45	0.77	0.0104	16.2	2.7778	-

	MOF/PVDF nanofibers film						
This work	**lamellae-crystal PA66 & FEP**	**153**	**7.35**	**0.67**	**10**	**15.3**	**2**

From the above obtained data, the sensitivity (S), which indicates the relationship between ΔV (change in voltage) and ΔF (change in force), can be calculated using the following formula,

$$S = \frac{\Delta V}{\Delta F}$$

Here, ΔV represents the change in voltage, while ΔF represents the change in force. By calculation, the sensitivity of the LC-TENG was determined to be 15.3 V/N. Table R2-1 shows a comparison between previously reported nylon-based sensors and those based on PA66 lamellae crystals. Although the previously reported nylon nanofiber-based triboelectric nanogenerator has shown great potential as a self-powered sensor, it has poor sensitivity. Addressing all, here we have fabricated PA66 lamellae crystal-based LC-TENG with enhanced sensitivity. This enhanced performance motivates the use of the fabricated LC-TENG as a self-powered sensor for motion, joint monitoring, etc.

References

(1) S. Bairagi, G. Khandelwal, X. Karagiorgis, S. Gokhool, C. Kumar, G. Min and D.M. Mulvihill, High-Performance Triboelectric Nanogenerators Based on Commercial Textiles: Electrospun Nylon 66 Nanofibers on Silk and PVDF on Polyester. *ACS Appl. Mater. Interfaces* 2022, **14**, 44591-44603.

(2) X. Guan, B. Xu, M. Wu, T. Jing, Y. Yang and Y. Gao, Breathable, washable and wearable woven-structured triboelectric nanogenerators utilizing electrospun nanofibers for biomechanical energy harvesting and self-powered sensing. *Nano Energy* 2021, **80**, 105549.

(3) S. Dong, F. Xu, Y. Sheng, Z. Guo, X. Pu and Y. Liu, Y. Seamlessly knitted stretchable comfortable textile triboelectric nanogenerators for E-textile power sources. *Nano Energy* 2020, **78**, 105327.

(4) G. J.Choi, S. H. Baek and I. K. Park, Synergetic Enhancement of Triboelectric Nanogenerators' Performance Based on Patterned Membranes Fabricated by Phase-Inversion Process. *Physica. Status. Solidi. (a)* 2021, **218**, 2000829.

(5) N. Sun, G. G. Wang, H. X. Zhao, Y.W. Cai, J. Z. Li, G. Z. Li, X. N. Zhang, B. L. Wang, J. C. Han, Y. Wang and Y. Yang, Waterproof, breathable and washable triboelectric nanogenerator based on electrospun nanofiber films for wearable electronics. *Nano Energy* 2021**, 90**, 106639.

(6) J. Qian, J. He, S. Qian, J. Zhang, X. Niu, X. Fan, C. Wang, X. Hou, J. Mu, W. Geng and X. Chou, A Nonmetallic Stretchable Nylon-Modified High Performance Triboelectric Nanogenerator for Energy Harvesting. *Adv. Funct. Mater.* 2019, **30**, 1907414.

(7) N. K. Das, M. Ravipati and S. Badhulika, Nickel Metal-Organic Framework/PVDF Composite Nanofibers based Self-Powered Wireless Sensor for Pulse Monitoring of Underwater Divers via Triboelectrically Generated Maxwell- Displacement Current. *Adv. Funct. Mater.* 2023, 2303288. DOI: 10.1002/adfm.202303288.